

The role of the self-interaction error in studying first principles chemisorption on graphene

Simone Casolo^{a*} and Espen Flage-Larsen^b, Ole Martin Løvvik^{b,c}, Gian Franco Tantardini^{a,d}

^a*Dipartimento di Chimica Fisica ed Elettrochimica,*

Università degli Studi di Milano, via Golgi 19, 20133 Milan, Italy.

^b*Department of Physics, University of Oslo, P.O. Box 1048 Blindern, NO-0316 Oslo, Norway*

^c*SINTEF, Materials and Chemistry, Forskningsvn. NO-0314 Oslo, Norway*

^d*CIMAINA, Interdisciplinary Center of Nanostructured Materials and Interfaces, University of Milan*

Adsorption of gaseous species, and in particular of hydrogen atoms, on graphene is an important process for the chemistry of this material. At the equilibrium geometry, the H atom is covalently bonded to a carbon that puckers out from the surface plane. Nevertheless the *flat* graphene geometry becomes important when considering the full sticking dynamics. Here we show how GGA-DFT predicts a wrong spin state for this geometry, namely $S_z=0$ for a single H atom on graphene. We show how this is caused by the self-interaction error since the system shows fractional electron occupations in the two bands closest to the Fermi energy. It is demonstrated how the use of hybrid functionals or the GGA+ U method can be used to retrieve the correct spin solution although the latter gives an incorrect potential energy curve.

I. INTRODUCTION

Thanks to its peculiar semi-metallic band structure, graphene is a very promising material for future silicon-free nano electronics [1, 2]. In particular, graphene's charge-carriers mobility is indeed extraordinarily high, with mean-free paths in the order of microns[3, 4]. However, for the fabrication of logic devices the absence of a band gap is a major issue since it does not allow a complete turn-off of the current, hence high on-off ratios[2, 5]. One straightforward possibility for graphene band-gap engineering is to use the adsorption of radicals or small molecules to create π defects, breaking the equivalence of its two sublattices. In this perspective several studies have been performed on isolated[6, 7], clusters[8–11] and even superlattices of adsorbates bonded on graphene, and most of them are based on the density functional theory (DFT). Among these hydrogen atoms adsorption is by far the most studied case, also because of the many implications in other fields[12, 13].

Hydrogen chemisorption dynamics on graphene is not yet completely understood. In the adiabatic picture when a H atom impinges on graphene and binds at its top site it induces one carbon atom to move out from the plane, “puckering” the surface. On the other hand, if the incoming species moves fast enough toward the graphene layer, sticking can occur faster than surface reconstruction; in this case the substrate can be considered as rigid. The planar geometry may thus play an importance role in the adsorption dynamics, and the accuracy of DFT calculations in this case is crucial in order to build reliable potential energy surfaces for quantum dynamics studies. In this article we analyze the spin properties of the substrate when a H atom is forced to chemisorb on a *flat*

graphene sheet. We show how the loss of spin polarization is a fictitious feature of semi-local generalized gradient approximation (GGA) functionals due to the self-interaction error (SIE). Then we will show how the correct ground state magnetization can be achieved using hybrid functional or GGA+ U approaches, even though the latter approach fails in reproducing the correct H-graphene potential energy curve.

II. COMPUTATIONAL METHODS

In brief, periodic density functional theory as implemented in the VASP package [14, 15] has been used throughout. A GGA-PBE functional was used and the plane wave basis set was limited to a 500 eV energy cutoff. For the inner electrons we rely on the frozen core approximation using PAW pseudo-potentials [16]. The reciprocal space was sampled by Γ centered k-point grids, whose meshes were chosen depending on the supercell size, in any case never more sparse than 6x6x1. The graphene unit supercells used here range from a 2x2 to a 5x5: all of them have a vacuum region along the c axis of 20 Å in order to guarantee a vanishing interaction between periodically repeated images. It has been shown recently that for hydrogen adsorption a 5x5 supercell is still not big enough to extract adsorption energies at meV accuracy [8], although this goes beyond the aim of this work. Further details about the computational setup can be found in ref.[8].

III. RESULTS AND DISCUSSION

When a radical species chemisorbs onto graphene or graphite surfaces the most favorable outcome is the formation of a covalent bond with one of the surface carbons, *i.e.* at a top site. The simplest case of radical

*Electronic address: simone.casolo@unimi.it

is a single (neutral) hydrogen atom. Applying Valence Bond (VB) arguments to this reaction one can predict that as the atom approaches the substrate plane it interacts with a π electron of graphene, triggering orbital re-hybridization of the C atom from a planar sp^2 to a partially tetrahedral sp^3 configuration [6, 7]. At long range the adsorbate - substrate interaction is purely repulsive since there is no unpaired electron on graphene available to bind hydrogen. At short range however a low-lying spin-excited state in which two π electrons lying on opposite, non-overlapping ends of a benzene ring would give rise to an attractive, barrierless interaction with the H $1s$ lone electron. Hence, an avoided crossing between these two doublet curves occurs giving rise to an activation barrier to chemisorption (see Fig.5 in ref.[8]). When the graphene sheet is allowed to reconstruct this process reads as a $sp^2 - sp^3$ orbital re-hybridization of the carbon involved in the bonding that turns partially tetrahedral, puckering out 0.6 \AA from the layer plane.

The graphene lattice is a bipartite system, made of two equivalent sublattices, each made of every second carbon atom. The equivalence of the two honeycomb sublattices is responsible for the particle-hole symmetry in graphene, and for the peculiar conical intersection at E_F between the valence and conduction bands [17]. A chemisorbed species creates a defect in the aromatic network, hence an imbalance between the number of occupied sites of the two π sublattices (n_A and n_B respectively). According to a theorem formulated by Inui *et. al.* within tight-binding theory, whenever an imbalance (vacancy) is introduced in a bipartite lattice this gives rise to $|n_A - n_B|$ zero-energy midgap states, localized on one sublattice only [18]. Moreover, following the second Lieb's theorem [19], since the total number of electrons is odd the total magnetization for non-metallic systems has to be $S^2 = |n_A - n_B|/2$. Thus, for a single defect $S_z=1/2$, or $1 \mu_B$.

DFT calculations confirm this picture: the hydrogen atom introduces a defect in one of the two sublattices, breaking one among the many aromatic bonds around the tetrahedral carbon. This implies that an unpaired electron can be delocalized by a "bond switching" process along the other sublattice, made of every second carbon atom. In the energy spectrum this reads as a flat band at the Fermi level *i.e.* in a midgap state occupied by one single spin projection only [8, 20].

According to previous studies [6, 7] we found at the GGA-DFT level that keeping the substrate planar thwarts the $sp^2 - sp^3$ re-hybridization; this is enough to weaken the attractive C-H interaction, but also to corrupt the system's aromatic character. Nevertheless, because the VB arguments concerning the crossing of two spin states hold, only a meta-stable C-H bond can form.

From our DFT calculations we notice how the total spin for H adsorbed on flat graphene is lower than expected at the local minimum geometry. In Fig.1 is shown the value of magnetization (left panel) along the adsorption path for several surface coverages, together with the total

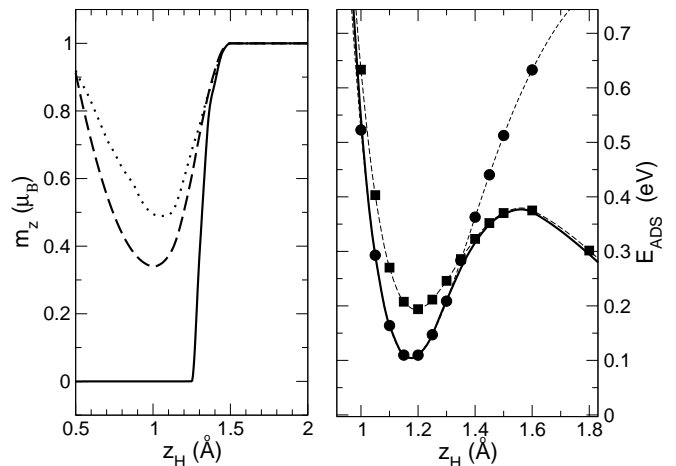


Figure 1: Left panel: total spin vs. distance from the surface for a H atom Adsorbing on flat graphene. The coverages are the following: $\Theta=0.031$ (full line), 0.055 (dashed) and 0.125 ML (dotted).

Right panel: adsorption potential curves for H (full line) together with the same curves for the spin unpolarized case (squares) and for the fixed magnetization $1 \mu_B$ (circles). The full line shows the adiabatic (non-constrained) curve. Zero energy here is set asymptotically away from graphene.

energies for the spin-polarized and unpolarized solutions (right panel). When the radical is far from the surface its magnetic moment is correctly $1 \mu_B$: this corresponds to an electron lying in the H $1s$ orbital, while graphene electronic structure remains intact. As the atom approaches the graphene layer along the normal direction, at a given critical height from the surface ($z_c(H) \simeq 1.25 \text{ \AA}$) the system's spin drops. The minimum value for the total spin depends upon the coverage. When coverage is low enough the spin is eventually quenched down to zero. Pushing the adsorbate closer to the carbon atom the magnetization tends to increase again. We tested that the same picture also holds for other small organic radicals with slightly different critical heights, weakly dependent upon the supercell size (coverage).

When comparing the adsorption curves computed with a magnetization fixed to 0 and $1 \mu_B$ as in Fig.1 (right panel), it is clear that the non-magnetic (non-polarized) solution becomes more stable than the magnetic one beyond the critical point z_c .

To a closer look (see Fig.2b) we notice that the occupied hydrogen s orbital and its (empty) affinity level get closer in energy when approaching graphene consistently with the Newns-Anderson model [21, 22]. Then around z_c they approach E_F , become degenerate and equally occupied by a fractional number of electrons. In the system's density of states, a gap opens at the point of the spin quenching together with the formation of a broad partially occupied peak at the Fermi energy, symmetric for both spin projections.

If the host were a metal, then spin-flip scattering between conduction electrons and a magnetic impurity might lead

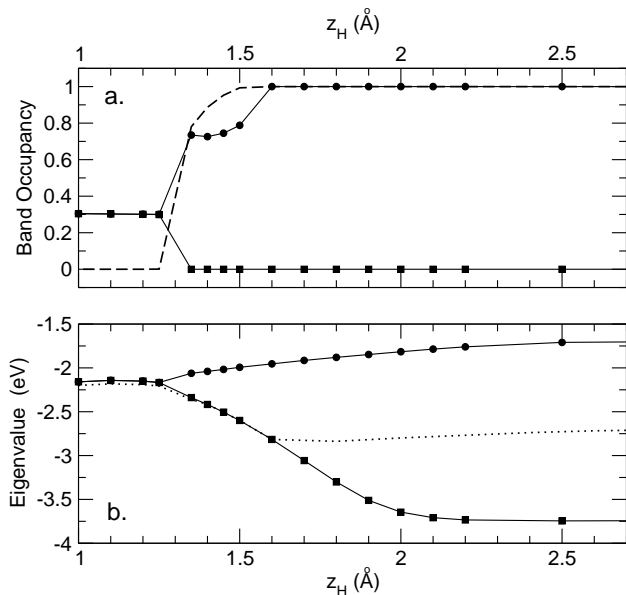


Figure 2: *a*: Occupancy for the spin up (circles) and spin down (squares) bands closest to E_F along the whole adsorption path. Dashed line: total magnetization (in μ_B). *b*: Eigenvalues for the bands shown above, the dotted line represents the value of the Fermi energy.

to a singlet ground state (Kondo effect). However in our case there is not a delocalized free-electron-gas-like surface state (a Shockley state) that is free to screen the impurity. Moreover the s electron does not belong to a localized orbital decoupled from the substrate such as for d metals. The Kondo effect is a many body feature that is not well described by DFT. Anyway this technique can describe correctly the spin quenching on metallic substrates, such as for a hydrogen atom impinging on Cu, Ag or Al(111) surfaces where this spin transition is a signature of non-adiabatic effects [23, 24].

We found that radical adsorption on planar graphene is a situation in which the (many-electron) self-interaction error (thereafter SIE, also known as delocalization error[25]) is particularly severe. Following the notation in ref[26] this is a chemical reaction with two centers ($m = 2$) and one electron ($n = 1$), since none of the electrons of graphene may be directly involved in bonding if they cannot re-hybridize to a tetrahedral sp^3 state. Systems with a fractional n/m ratio are also known to exhibit of large static electronic correlation [27].

A well known system with $n/m = 1/2$ is the H_2^+ molecular ion dissociation. When the two atoms are far apart both the local density approximation (LDA) and GGA local functionals give as the most stable ground state half of an electron on each of the two degenerate atomic orbitals, which is physically not correct. Asymptotically the orbitals on the two fragments are degenerate, so this fractional occupation solution should be degenerate with any other possible electronic arrangement such as one filled and one empty orbital [28]. Fractional charge (and spin)

on the two fragments is due to the over-delocalization that is a direct consequences of the SIE. Indeed the LDA and GGAs functionals are designed to correctly reproduce the system’s total density and the on-top pair density, but fail in pathological systems to reproduce spin densities because of the SIE [29, 30]. This non-integer orbital occupation is directly related to the break down of sum rules over the exchange hole density $n_x(\mathbf{r}, \mathbf{r}')$

$$\int n_x(\mathbf{r}, \mathbf{r}') d\mathbf{r}' = \sum_{\alpha, \sigma} f_{\alpha, \sigma} \frac{n_{\alpha, \sigma}(\mathbf{r})}{n(\mathbf{r})} \quad (1)$$

that when the orbital occupation f becomes fractional sums to a value within larger than the correct -1. Thus local functionals give an energy whose behaviour is convex for a fractional number of electrons instead of being linear according to Janak theorem [31]. For this reason for open systems a delocalized situation with fractional charge turns out to be more favored [25].

For H adsorbed on flat graphene the spin quenching is similarly due to a fractional spin situation: the “splitting” of one electron in two different *degenerate* bands (originating from H s and C p_z), with opposite spin projections (see Fig.2). Here the occupation number in these bands can fluctuate, a sign that SIE is particularly severe [32]. This picture is confirmed by the convex behaviour of the system energy for fractional band occupation as shown in Fig.3, obtained by constraining a given occupation within the two bands. Note that two degenerate orbitals every arrangement of electrons (even for fractional numbers) should be perfectly degenerate. In this case however, the energy minimum lays exactly at the unpolarized solution: 0.5 occupancy of the two bands.

Another indication of the SIE is the worsening of the spin quenching at low coverages, hence for larger and larger super-cells, as shown before in Fig.1. With the SIE being cause of the delocalization, the fractional occupancy might not be maximal when the unit cell is not large enough to accommodate all the delocalized electron density [33].

A major difference with the H_2^+ prototype case is that here there is no fractional spin asymptotically for H since the involved orbitals here lay far below graphene Fermi energy. For other and more electronegative monovalent species such as F and OH fractional charges appear also asymptotically, similarly to the case of dissociations of heteronuclear diatomics [34].

To prove further that the failure in representing the total spin of the system comes from the approximate nature of the density functionals we tested the performances of a (non-local) hybrid functional. Hybrid functionals combine the GGA exchange and correlation term (convex for fractional electron number) with the Hartree-Fock (HF) “exact” exchange term. Since HF energies have instead a concave behaviour for fractional electron numbers they often yield over-corrected results [33]. For this reason the use of a fraction (usually one fourth) of exact exchange to correct the DFT E_{xc} functional gives much better results, at least for non-metallic systems [35]. We then chose the

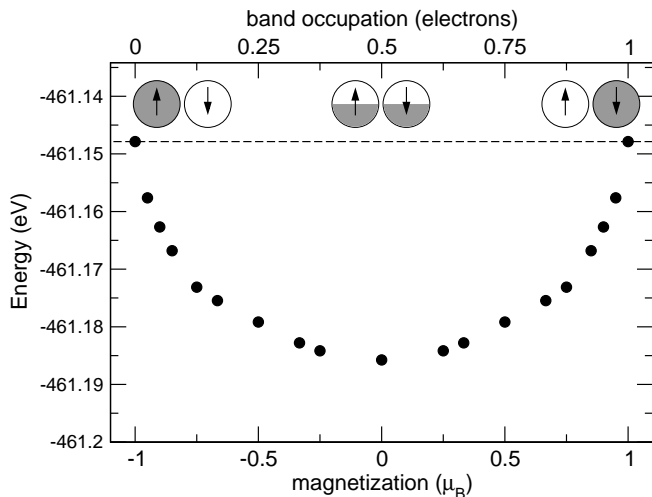


Figure 3: Calculated total energy vs. magnetization for one H atom adsorbed on flat graphene. When the magnetization is -1 or $1 \mu_B$ one of the two degenerate bands is occupied while the other is empty. For the non-polarized, $0 \mu_B$, case both bands are occupied by half of an electron each. The full line represents the correct degenerate behaviour for fractional electron numbers; filled circles are the GGA-DFT results.

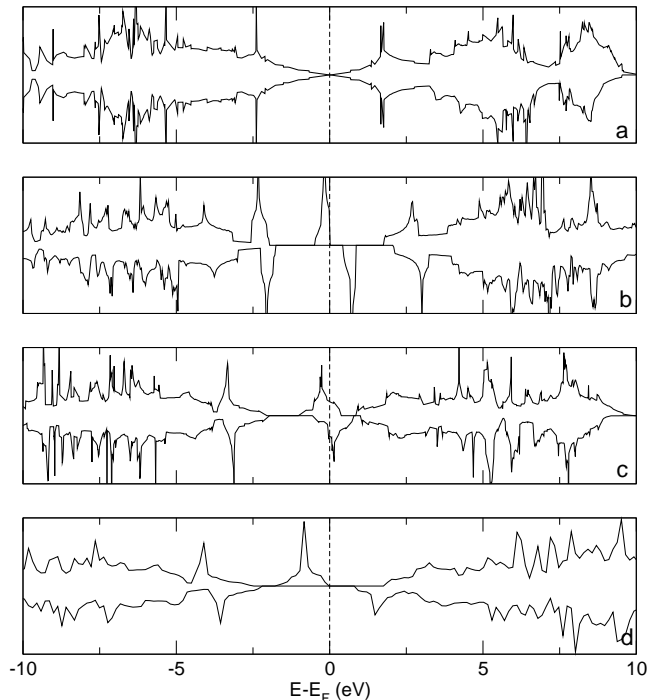


Figure 4: Density of states for the H-flat graphene system obtained for a 2×2 supercell. PBE results for: a) clean graphene, b) H adsorbed on reconstructed (puckered) graphene, c) H adsorbed on flat graphene ($M=0 \mu_B$). Hybrid-PBE0 results ($1 \mu_B$) are shown in d) for comparison. As a guide to the eye the Fermi energy is shown as dashed vertical line.

PBE0 functional, which mixes 25% of HF with 75% of PBE exchange, and uses the full PBE correlation[36]:

$$E_{xc}^{PBE0} = E_{xc}^{PBE} + 0.25(E_x^{HF} - E_x^{PBE})$$

Hybrid functionals are orbital dependent, *i.e.* non-local in space: this is a major issue when employing plane wave codes where the number of orbitals depends upon the supercell volume. The computational effort needed for this kind of calculations is thus much larger compared to GGA. Hence we could not reach low coverages, restricting our system to a 2×2 supercell ($\Theta=0.125$ ML). Within hybrid functional DFT the system's total spin for H on flat graphene layer is $1 \mu_B$ ($S_z=1/2$), and the associated spin density is correctly localized on one sublattice only. A comparison between the density of states computed with PBE and PBE0 is shown in Fig.4. GGA can represent pretty well the adiabatic chemisorption mechanism, namely the band gap opening and the zero energy midgap state that splits by the exchange interaction into a filled and an empty states with opposite spin (Fig4a and b). For the flat geometry, GGA gives a broad feature straddling across the Fermi energy (Fig4c). For larger supercells (at lower coverages) the peak becomes fully symmetric for the two spin projections, giving rise to the un-polarized state. On the other hand PBE0 can reproduce well the occupied midgap state. As it is widely known standard DFT tend to underestimate the band gaps, again due to the SIE[37]: for this reason the PBE0 band-gap is about 50% larger than that of PBE.

It has also been proposed that an "on site" repulsion term such as in the LSDA+ U [38] approach can help to control the SIE in case of fractional occupation [39]. The on site Coulomb term U acts as a penalty for the occupation of the two degenerate bands at the Fermi energy, and can thus reproduce the correct ground state. Note that LSDA+ U and GGA(PBE)+ U , as implemented here, give practically identical results in this case. This approach is much less computationally expensive than the hybrid functionals, so we could study the full adsorption path. As for PBE0 the total magnetization is $1 \mu_B$ at every C-H distance, and the spin density correctly is localized either on the H atom or on one graphene sublattice. From our tests a Coulomb interaction of 15 eV was enough to retrieve the correct ground state spin: a value not far from 20.08 eV, already successfully used to describe carbon π electrons in similar approaches [40, 41].

We would like to stress that the GGA+ U approach is not a rigorous way to avoid self interaction, and hence some care has to be taken when interpreting these results. While it is relatively easy to predict which has to be the correct total spin of the system upon physical arguments, it is more challenging to judge the quality of total energies. Indeed, it can be seen from Fig.5 that the effect of the on-site U term is to lower the activation barrier at z_c making the adsorption curve to a fully repulsive interaction. Being the chemisorption potential energy curve for H on graphene the result of the interplay of two an attractive and a repulsive doublet spin states

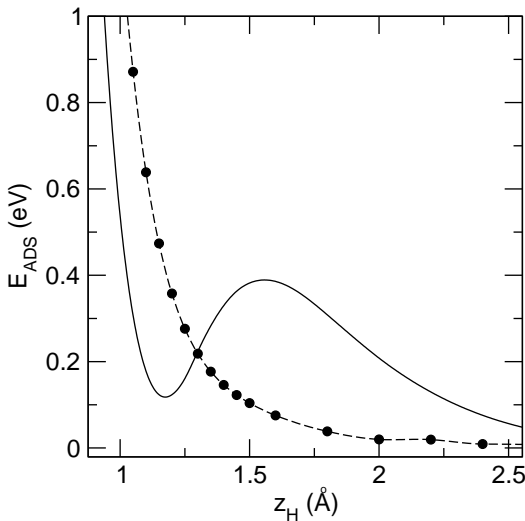


Figure 5: Comparison between GGA (full line) and GGA+ U (dashed line) potential energy curves along the adsorption path. Note how GGA+ U do not show the correct activation barrier arising from the avoided crossing of the two curves shown in the right panel of Fig.1

their avoided crossing has necessarily to occur. For this reason the GGA+ U results, despite showing the correct magnetization, cannot represent the correct H-graphene

interaction in all its aspects.

IV. CONCLUSIONS

The chemisorption of a hydrogen atom onto a flat graphene sheet has been studied within semi-local GGA-DFT. Contrary to the adiabatic case the substrate $sp^2 - sp^3$ re-hybridization is limited, so adsorbate and substrate bands become degenerate at a given critical C-H distance, z_c , where the total magnetization drops to zero. This spin transition is due to a fractional spin configuration: a fictitious effect induced by the self-interaction error. To overcome this issue it is possible to use a hybrid functional such as PBE0. The GGA+ U approach can reproduce the correct magnetization, but leads to qualitatively incorrect potential energy curves.

V. ACKNOWLEDGMENTS

The authors thank the NOTUR consortium for providing computational resources. S. C. acknowledges the University of Oslo for the hospitality during his stay and Rocco Martinazzo and George Darling for the many useful comments.

-
- [1] A. H. Castro Neto, F. Guinea, N. M. R. Peres, K. S. Novoselov, and A. K. Geim, *Rev. Mod. Phys.* **81**, 109 (2009).
 - [2] P. Avouris, Z. Chen, and V. Perebeinos, *Nat. Nanotech.* **2**, 605 (2007).
 - [3] K. Bolotin, K. Sikes, Z. Jang, M. Klima, G. Fudenberg, J. Hone, P. Kim, and H. L. Stromer, *Solid State Commun.* **143**, 351 (2008).
 - [4] F. Schedin, A. K. Geim, S. V. Morozov, E. W. Hil, P. Blake, M. I. Katsnelson, and K. S. Novoselov, *Nat. Mater.* **6**, 652 (2007).
 - [5] K. Novoselov, *Nat. Mater.* **6**, 720 (2007).
 - [6] L. Jeloica and V. Sidis, *Chem. Phys. Lett.* **300**, 157 (1999).
 - [7] X. Sha and B. Jackson, *Surf. Sci.* **496**, 318 (2002).
 - [8] S. Casolo, O. M. Løvvik, R. Martinazzo, and G. F. Tattardini, *J. Chem. Phys.* **130**, 054704 (2009).
 - [9] L. Hornekær, Ž. Šljivančanin, W. Xu, R. Otero, E. Rauls, I. Stensgaard, E. Lægsgaard, B. Hammer, and F. Besenbacher, *Phys. Rev. Lett.* **96**, 156104 (2006).
 - [10] L. Hornekær, E. Rauls, W. Xu, Ž. Šljivančanin, R. Otero, I. Stensgaard, E. Lægsgaard, B. Hammer, and F. Besenbacher, *Phys. Rev. Lett.* **97**, 186102 (2006).
 - [11] D. W. Boukhvalov, M. I. Katsnelson, and A. I. Lichtenstein, *Phys. Rev. B* **77**, 035427 (2008).
 - [12] R. J. Gould and E. E. Salpeter, *Astrophys. J.* **138** (1963).
 - [13] D. Hollenbach and E. E. Salpeter, *J. Chem. Phys.* **53**, 79 (1970).
 - [14] G. Kresse and J. Hafner, *Phys. Rev. B* **49**, 14251 (1994).
 - [15] G. Kresse and J. Hafner, *Phys. Rev. B* **47**, 558 (1993).
 - [16] P. E. Blöchl, *Phys. Rev. B* **50**, 17953 (1994).
 - [17] J. C. Slonczewski and P. R. Weiss, *Phys. Rev.* **109**, 272 (1958).
 - [18] M. Inui, S. A. Trugman, and E. Abrahams, *Phys. Rev. B* **49**, 3190 (1994).
 - [19] E. H. Lieb, *Phys. Rev. Lett.* **62**, 1201 (1989).
 - [20] T. O. Wehling, M. I. Katsnelson, and A. I. Lichtenstein, *Phys. Rev. B* **80**, 085428 (2009).
 - [21] P. W. Anderson, *Phys. Rev.* **124**, 41 (1961).
 - [22] D. M. Newns, *Phys. Rev.* **178**, 1123 (1969).
 - [23] M. Lindenblatt and E. Pehlke, *Phys. Rev. Lett.* **97**, 216101 (2006).
 - [24] M.S., Mizielinski, D. Bird, M. Persson, and S. Holloway, *Surf. Sci.* **602**, 2617 (2008).
 - [25] A. J. Cohen, P. Mori-Sanchez, and W. Yang, *Science* **321**, 792 (2008).
 - [26] O. Gritsenko, B. E. P. R. T. Schipper, and E. J. Baerends, *J. Phys. Chem. A* **104**, 8558 (2000).
 - [27] Y. Zhang and W. Yang, *J. Chem. Phys.* **109**, 2604 (1998).
 - [28] P. Mori-Sanchez, A. Cohen, and W. Yang, *Phys. Rev. Lett.* p. 066403 (2009).
 - [29] K. Burke, J. P. Perdew, and M. Ernzerhof, *J. Chem. Phys.* **109**, 3760 (1998).
 - [30] J. P. Perdew, A. Savin, and K. Burke, *Phys. Rev. A* **51**, 4531 (1995).
 - [31] G. B. Perdew, R. G. Parr, M. Levy, and J. L. Balduz Jr., *Phys. Rev. Lett.* **49**, 1691 (1982).
 - [32] J. P. Perdew, A. Ruzsinsky, G. I. Csonka, O. A. Vydrov,

- and G. E. Scuseria, Phys. Rev. A **76**, 040501 (2007).
- [33] P. Mori-Sanchez, A. Cohen, and W. Yang, Phys. Rev. Lett. **100**, 146401 (2008).
- [34] A. Ruzsinszky, J. P. Perdew, G. I. Csonka, O. A. Vydrov, and G. E. Scuseria, J. Chem. Phys. **125**, 194112 (2006).
- [35] M. Marsman, J. Paier, A. Stroppa, and G. Kresse, J. Phys.: Condens. Matter **20**, 064201 (2008).
- [36] C. Adamo and V. Barone, J. Chem. Phys. **110**, 6158 (1999).
- [37] A. Cohen, P. Mori-Sanchez, and W. Yang, Phys. Rev. B **77**, 115123 (2008).
- [38] S. L. Dudarev, G. A. Botton, S. Y. Savrasov, C. J. Humphreys, and A. P. Sutton, Phys. Rev. B **57**, 1505 (1998).
- [39] M. Cococcioni and S. de Gironcoli, Phys. Rev. B **71**, 035105 (2005).
- [40] T. G. Pedersen, Phys. Rev. B **69**, 075207 (2004).
- [41] T. Pedersen, C. Flindt, J. Pedersen, N. Mortensen, A. P. Jauho, and K. Pedersen, Phys. Rev. Lett. **100**, 136804 (2008).